J. Fluid Mech. (1973), *vol.* 58, *part* 3, *pp.* 561–579
Printed in Great Britain

A numerical method for integrating the unsteady boundary-layer equations when there are regions of backflow

By J. H. PHILLIPS AND R. C. ACKERBERG
Polytechnic Institute of Brooklyn, Graduate Center, Farmingdale, New York 11735

(Received 23 September 1971 and in revised form 7 November 1972)

A numerical method for integrating the unsteady two-dimensional boundary-layer equations using a second-order-accurate implicit method, which allows for arbitrary mesh spacing in the space and time variables, is developed. A unique feature of the method is the use of an asymptotic solution valid at the downstream end of the integration mesh which permits backflow to be taken into account. Newton's iterative technique is used to solve the nonlinear finite-difference equations at each computation step, using a rapid algorithm for solving the resulting linearized equations. The method is applied to a flow which is periodic in time and contains regions of backflow. The numerical computations are compared with known numerical and asymptotic solutions and the agreement is excellent.

1. Introduction

This paper is concerned with numerical solutions of the unsteady laminar boundary-layer equations for flows over a semi-infinite flat plate which is parallel to the free stream. The fluid velocity outside the boundary layer is assumed uniform and a periodic function of time. The periodicity gives rise to regions of backflow near the wall, and by using an asymptotic solution, valid at the downstream end of the integration mesh, a method is devised for allowing the backflow to influence the motion upstream. These problems arise in the flow over a helicopter blade and are related to the fluid motion in the human aorta.

The numerical method presented here is a fast and versatile second-order-accurate implicit technique which allows for arbitrary mesh spacing in the space and time variables. The nonlinear finite-difference equations at each computation step are solved using Newton's iterative method, and a rapid algorithm for solving the resulting linearized equations is given. Although no results are presented here for flows without backflow, the method has also been used in these cases with excellent results (Phillips 1972). Certain similarities exist between the numerical method presented here and that of Hall (1969*b*). The main differences are as follows. (i) The method presented here allows for a variable mesh size across the boundary layer, making it especially suitable for studying double boundary-layer structures. (ii) Our method solves the nonlinear finite-difference equations by Newton's technique rather than by a fixed-point method.

(iii) The linear system of equations which arise with each Newton iteration are solved using an algorithm rather than by factorization into upper and lower triangular matrices. A considerable amount of computing time is saved by this method because it is not necessary to operate on the zero elements which appear in the matrices.

A motion is considered for which the fluid velocity outside the boundary layer is a periodic function of time $\bar{t}$ given by $\overline{U}_e = \overline{U}_0 + \overline{U}_1 \sin \bar{\omega}\bar{t}$, where $\bar{\omega}$ is the frequency, and with $|A| = |\overline{U}_1/\overline{U}_0| < 1$, so that no backflow occurs at the leading edge. The motion is started impulsively from rest, and only periodic solutions which would result for $t \to \infty$ are sought. It is assumed that unique periodic solutions exist, independent of initial conditions. This is tested numerically by choosing different initial conditions.

This problem has been considered by several authors (e.g. Lighthill 1954; Ackerberg & Phillips 1972 and their references) when A is small (hereafter referred to as the 'small parameter' solution). For such cases the nonlinear partial differential equations can be reduced to linear partial differential equations using standard perturbation techniques. For larger values of $|A| < 1$ and $\bar{\omega} \to \infty$, the problem was considered by Lin (1957) and Gibson (1957). Using time averages of the governing equations, Lin was able to separate the boundary-layer solution into a steady and fluctuating part, and he deduced the double boundary-layer structure valid far downstream, which, to first order, has an inner layer which corresponds to a Stokes shear-wave motion, while the outer layer is a modified Blasius flow which carries the mean flow downstream. Gibson also studied this problem when $\overline{U}_e$ is a slowly varying function of time ($\bar{\omega}$ small). His analysis was confined to the case in which $|A| \ll 1$.

Numerical solutions are obtained and compared with a co-ordinate expansion, valid near the leading edge of the plate, and with the 'small parameter' solution of Ackerberg & Phillips (1972). All results are in good agreement. Attempts were also made to compare the numerical solutions with asymptotic solutions valid far downstream once periodicity had been established (Phillips, private communication; Pedley 1972). However, the values of x and t required were so large that the calculation was prohibitive in terms of computing machine time and storage. Calculations are also made for the case when the fluid velocity near the wall is directed upstream. The results indicate that regions of backflow for unsteady boundary-layer motions of this type do not cause any apparent singularity in the solution at the point of zero skin friction. This observation is in agreement with current views regarding separation (Stewartson 1960; Sears & Telionis 1971), and it emphasizes the fact that the single condition $[\partial\bar{u}/\partial\bar{y}]_{\bar{y}=0} = 0$ is not sufficient for signalling separation of unsteady flows.

A unique feature of our technique is the use of a Rayleigh solution, valid at some finite distance downstream of the leading edge, to compute the flow field when there are regions of backflow. The theoretical basis for this method is a generalization of a result of Stewartson (1951) that information regarding the existence of the leading edge travels downstream at finite velocity, say $\overline{U}_{eM}$; thus, if $\bar{t}$ is the time measured from the initiation of the motion, the fluid at stations $\bar{x} > \overline{U}_{eM}\bar{t}$ is unaware of the leading edge and undergoes Rayleigh motion corre-

sponding to an infinite plate with the imposed velocity $\overline{U}_e(\bar{t})$ (see the discussion on p. 565). To use this result, the x mesh along the plate is expanded with time so that the farthest x station from the leading edge is always situated in the Rayleigh flow. When backflow occurs, the downstream flow conditions will be known and may be used to influence and compute the upstream flow by modifying the finite-difference equations. After some time the number of mesh points in the x direction will be quite large, but as periodicity (in time) is established at upstream stations, the x mesh can be contracted by moving the initial x station downstream, provided that sufficient computer storage is available to retain the velocity and shear values at the new initial station for a full period. The contraction procedure was not used here owing to lack of storage.

In § 2, the problem is non-dimensionalized and formulated mathematically. The numerical method and the particular modifications to account for backflow are discussed in § 3. The application to the periodic flow problem is considered. in § 4.

2. Mathematical formulation

Consider the flow of a viscous incompressible fluid over a semi-infinite flat plate. The fluid velocity $\overline{U}_e(\bar{t})$ at large distances is a prescribed periodic function of time $\bar{t}$ with frequency $\overline{\omega}$ (see figure 1).† The co-ordinate system is chosen with the origin located at the leading edge and the $\bar{x}$ axis along the plate with $\bar{x}$ measured positively downstream. The $\bar{y}$ axis is normal to the plate and directed into the fluid. Two Reynolds numbers may be defined: $Re_1 = \overline{U}_0\bar{x}/\bar{\nu}$ and $Re_2 = \overline{U}_0^2/(\overline{\omega}\bar{\nu})$, where $\overline{U}_0$ is the mean velocity, associated with $\overline{U}_e(\bar{t})$, and defined by

$$\overline{U}_0 = (\overline{\omega}/2\pi)\int_{\bar{t}}^{\bar{t}+2\pi/\overline{\omega}} \overline{U}_e(\bar{t})\,d\bar{t}. \tag{2.1}$$

Here $\bar{\nu}$ is the kinematic viscosity. Both Re_1 and Re_2 are assumed large so that the Prandtl boundary-layer equations can be used, except in a small neighbourhood of the leading edge where the Navier–Stokes equations are necessary.

Denoting dimensional variables by bars, the following non-dimensional dependent and independent variables are introduced:

$$\left.\begin{aligned} u &= \bar{u}/\overline{U}_e(\bar{t}), \quad v = \bar{v}\,Re_1^{\frac{1}{2}}/(\overline{U}_e\overline{U}_0)^{\frac{1}{2}}, \quad x = \overline{x\omega}/\overline{U}_0, \\ \eta &= \bar{y}[\overline{U}_e(\bar{t})/\overline{\nu x}]^{\frac{1}{2}}, \ \ddagger \quad t = \bar{t}\overline{\omega}, \quad U_e(t) = \overline{U}_e(\bar{t})/\overline{U}_0. \end{aligned}\right\} \tag{2.2}$$

We denote partial differentiation by subscripts and put $dU_e/dt = \dot{U}_e$; the boundary-layer equations for conservation of mass and x momentum may be written as

$$xu_x - \tfrac{1}{2}\eta u_\eta + v_\eta = 0 \tag{2.3}$$

and

$$x[u_t + U_e^{-1}\dot{U}_e(u + \tfrac{1}{2}\eta u_\eta - 1) + U_e u u_x] + U_e(v - \tfrac{1}{2}\eta u)\,u_\eta - U_e u_{\eta\eta} = 0. \tag{2.4}$$

† Flows for which $\overline{U}_e(\bar{t})$ is constant can also be considered a limiting case of a periodic flow. It can be shown that in this case $\overline{\omega}$ will not appear in the solution (see Phillips 1972).

‡ This transformation is not one–one at $\bar{x} = 0$ since any $\bar{y} > 0$ maps onto $\eta = \infty$.

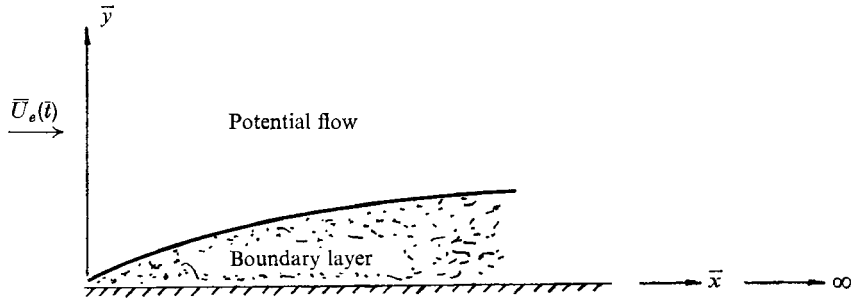

FIGURE 1. Flow geometry.

2.1. *Boundary conditions*

The no-slip condition at the wall requires

$$u(x,0,t) = 0 = v(x,0,t). \tag{2.5}$$

At the edge of the boundary layer the velocity must satisfy

$$u(x,\eta,t) \to 1 \quad \text{for} \quad \eta \to \infty. \tag{2.6}$$

2.2. *Initial conditions*

Initial conditions are required in both x and t. If we put $x = 0$ in the governing equations, we find that for the co-ordinate system used here the equations have lost their parabolic character in x and we are not free to impose an arbitrary initial condition. Thus, at $x = 0$, we require

$$u(0,\eta,t) = R'(\eta), \tag{2.7}$$

where $R(\eta)$, the Blasius solution, satisfies

$$R''' + \tfrac{1}{2}RR'' = 0, \quad R(0) = 0 = R'(0), \quad R'(\eta) \to 1 \quad \text{for} \quad \eta \to \infty. \tag{2.8}$$

Primes denote differentiation with respect to η and we should note that $R(\eta)$ is a solution of (2.3)–(2.6) when $x \equiv 0$.

At $t = 0$ we require

$$u(x,\eta,0) = u_0(x,\eta). \tag{2.9}$$

Initial conditions for v are not necessary since neither derivatives of v with respect to x nor t appear in the governing equations. The boundary and initial conditions given above are expected to be sufficient to determine a solution of the equations in normal situations.

2.3. *Downstream property of the flow*

Stewartson (1951) studied the motion of a flat plate, with a sharp leading edge, set impulsively into motion with uniform velocity $\bar{U}$. He showed that if $\bar{U}\bar{t} < \bar{x}$, where $\bar{x}$ is the distance measured downstream from the leading edge, the solution is independent of the initial condition at $\bar{x} = 0$. Since this problem is equivalent to one in which the fluid is impulsively set into motion and the plate is fixed, we infer that information concerning the existence of the leading edge passes

downstream from the leading edge at the maximum velocity within the boundary layer.

In the case of periodic boundary-layer flows there are usually times, say $\bar{t}_1$, during which there are overshoots of velocity within the layer where

$$\bar{u}(\bar{x}, \bar{y}, \bar{t}_1) > \bar{U}_e(\bar{t}_1).$$

However, if we formally extend the well-known maximum principle for linear parabolic partial differential equations (see Tikhonov & Samarskii 1963, p. 206) to include the present case, we conclude that $\bar{u} \leqslant \max \bar{U}_e(\bar{t})$, $\bar{t} \in [0, \infty)$, say $\bar{U}_{eM}$. Thus the solution for $\bar{x} \geqslant \bar{t}\bar{U}_{eM}$ (i.e. $x \geqslant tU_{eM}$) is independent of conditions at $\bar{x} = 0$, and corresponds to a Rayleigh solution with $\bar{U}_e(\bar{t})$ prescribed, i.e.

$$\bar{u}_{\bar{t}} = \dot{\bar{U}}_e + \bar{\nu}\bar{u}_{\bar{y}\bar{y}} \quad (0 \leqslant \bar{t} < \infty,\ 0 \leqslant \bar{y} < \infty),$$

$$\bar{v}(\bar{y}, \bar{t}) \equiv 0,$$

with $\bar{u}(\bar{y}, 0)$ prescribed and

$$\bar{u}(0, \bar{t}) = 0, \quad \bar{u}(\bar{y}, \bar{t}) \to \bar{U}_e(\bar{t}) \quad \text{for} \quad \bar{y} \to \infty.$$

This result does not influence the solution when there is no backflow. However, it is vital to use this information in the formulation when regions of backflow occur, since in that case the last downstream station of the region of integration cannot be computed using the numerical technique to be proposed. This will be discussed in more detail in § 3.5.

3. Numerical procedure

3.1. *Equations to be integrated*

For large values of x a double boundary layer is expected when the flow at the edge of the boundary layer is oscillatory. Thus, a numerical method which allows for variable mesh spacing in the y (or η) direction is desirable to achieve better resolution in the boundary layer. Keller & Cebeci (1971) have proposed a second-order-accurate implicit technique for steady flows with this feature and it is used here with some modifications.

First, we introduce a new dependent variable $w = u_\eta$. This substitution transforms the boundary-layer equations into the following system of first-order partial differential equations:

$$xu_x - \tfrac{1}{2}\eta w + v_\eta = 0, \tag{3.1}$$

$$x[u_t + (\dot{U}_e/U_e)(u + \tfrac{1}{2}\eta w - 1) + U_e u u_x] + U_e(v - \tfrac{1}{2}\eta u)w - U_e w_\eta = 0 \tag{3.2}$$

and

$$w - u_\eta = 0. \tag{3.3}$$

The integration will be performed in planes t = constant starting at $t = 0$, and within each t plane along the lines x = constant starting at $x = 0$ and proceeding downstream.

3.2. *Integration mesh*

Introduce the following grid (see figure 2). Let the index k ($\geqslant 1$) denote the position along the t axis with k increasing as t increases. The initial conditions in t are applied in the plane $k = 1$. Let the index i denote position along the

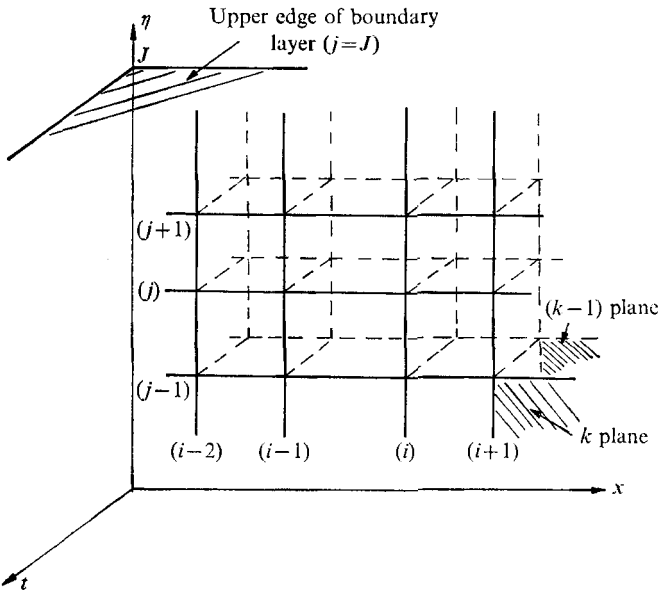

FIGURE 2. Integration mesh.

x axis with $i = 1$ for the plane $x = 0$. For each t plane let $i = I$ denote the downstream end of the region of computation. Let the index j denote the position along the η axis with $j = 1$ for $\eta = 0$ and $j = J$ for the upper edge of the boundary layer. Define the vector $(\delta x_i, \delta\eta_j, \delta t_k)$ such that

$$(\delta x_i, \delta\eta_j, \delta t_k) = (x_i, \eta_j, t_k) - (x_{i-1}, \eta_{j-1}, t_{k-1}).$$

For each computation it is necessary to fix the x_i and η_j arrays at the start with any desirable variations in δx_i and $\delta\eta_j$. During the course of computation δt_k may be changed at any step and any new x_i grid lines, which may be introduced at the downstream end of the grid, may have arbitrary spacing.

3.3. *Numerical integration*

Points at the leading edge of the plate ($i \equiv 1, 1 \leqslant j \leqslant J, k \geqslant 1$). The initial condition in x, equation (2.7), is satisfied by putting

$$u(x_1, \eta_j, t_k) = R'(\eta_j) \quad (1 \leqslant j \leqslant J, k \geqslant 1). \tag{3.4}$$

The change of dependent variables introduced in § 3.1 requires that we also specify

$$w(x_1, \eta_j, t_k) = R''(\eta_j) \quad (1 \leqslant j \leqslant J, k \geqslant 1). \tag{3.5}$$

Wall points ($i \geqslant 1, j \equiv 1, k \geqslant 1$). The boundary conditions (2.5) are satisfied by putting

$$u(x_i, \eta_1, t_k) = v(x_{i-\frac{1}{2}}, \eta_1, t_{k-\frac{1}{2}}) = 0 \quad (i, k \geqslant 1). \tag{3.6}$$

Points at the edge of the boundary layer ($i \geqslant 1, j \equiv J, k \geqslant 1$). The boundary condition (2.6) is satisfied by putting

$$u(x_i, \eta_J, t_k) = 1 \quad (i, k \geqslant 1). \tag{3.7}$$

By using the similarity variable η, based on the mean flow, the thickness of the boundary layer is expected to be nearly constant and (3.7) is sufficiently accurate. In other applications it may be desirable to use an asymptotic expansion in place of (3.7) (see Ackerberg & Phillips 1973; Phillips 1972).

Interior points ($i \geqslant 2$, $2 \leqslant j \leqslant J-1$, $k > 1$). To make the computations accurate to second order in the mesh spacings, (3.1) and (3.2) are satisfied at each intermediate mesh point $(p,q,r) = (i-\frac{1}{2}, j-\frac{1}{2}, k-\frac{1}{2})$ and (3.3) at each intermediate mesh point (i,q,k). Thus, u and w are computed at the points (i,j,k) while v is computed at the points (p,j,r). A simple average will determine v, with second-order accuracy, at the points (i,j,k). Since two types of situation occur, one with backflow, the other without, it is necessary to apply the numerical technique differently in each case. This difference, however, will affect only those terms in the finite-difference equations which arise from a previously computed t plane and a notation is introduced to represent these quantities symbolically so that we may discuss both situations at once. More details will be given in each particular case. To approximate velocities and derivatives in (3.1)–(3.3), we introduce the second-order-accurate notation

$$(x', \eta', t') = (x - \tfrac{1}{2}\delta x,\ \eta - \tfrac{1}{2}\delta\eta,\ t - \tfrac{1}{2}\delta t),$$

$$u(x',\eta',t') \approx \tfrac{1}{8}(u_{i,j,k} + u_{i,j-1,k}) + L_1 \equiv (u)_{p,q,r}, \tag{3.8a}$$

$$u_t(x',\eta',t') \approx (4\delta t_k)^{-1}(u_{i,j,k} + u_{i,j-1,k}) + L_2 \equiv (u_t)_{p,q,r}, \tag{3.8b}$$

$$u_x(x',\eta',t') \approx (4\delta x_i)^{-1}(u_{i,j,k} + u_{i,j-1,k}) + L_3 \equiv (u_x)_{p,q,r}, \tag{3.8c}$$

$$w(x',\eta',t') \approx \tfrac{1}{8}(w_{i,j,k} + w_{i,j-1,k}) + L_4 \equiv (w)_{p,q,r}, \tag{3.8d}$$

$$w_\eta(x',\eta',t') \approx (4\delta\eta_j)^{-1}(w_{i,j,k} - w_{i,j-1,k}) + L_5 \equiv (w_\eta)_{p,q,r}, \tag{3.8e}$$

$$v(x',\eta',t') \approx \tfrac{1}{2}(v_{p,j,r} + v_{p,j-1,r}) \equiv (v)_{p,q,r}, \tag{3.8f}$$

$$v_\eta(x',\eta',t') \approx \delta\eta_j^{-1}(v_{p,j,r} - v_{p,j-1,r}) \equiv (v_\eta)_{p,q,r}, \tag{3.8g}$$

$$u_\eta(x,\eta',t) \approx \delta\eta_j^{-1}(u_{i,j,k} - u_{i,j-1,k}) \equiv (u_\eta)_{i,q,k}, \tag{3.8h}$$

$$w(x,\eta',t) \approx \tfrac{1}{2}(w_{i,j,k} + w_{i,j-1,k}) \equiv (w)_{i,q,k}. \tag{3.8i}$$

The terms L_s ($s = 1$–5) are given by

$$L_1 = \tfrac{1}{8}(u_{i-1,j,k} + u_{i-1,j-1,k}) + \tfrac{1}{2}u_{p,q,k-1},$$

$$L_2 = \delta t^{-1}[\tfrac{1}{4}(u_{i-1,j,k} + u_{i-1,j-1,k}) - u_{p,q,k-1}],$$

$$L_3 = -(4\delta x_i)^{-1}(u_{i-1,j,k} + u_{i-1,j-1,k}) + \tfrac{1}{2}(u_x)_{p,q,k-1},$$

$$L_4 = \tfrac{1}{8}(w_{i-1,j,k} + w_{i-1,j-1,k}) + \tfrac{1}{2}w_{p,q,k-1},$$

$$L_5 = (4\delta\eta_j)^{-1}(w_{i-1,j,k} - w_{i-1,j-1,k}) + \tfrac{1}{2}(w_\eta)_{p,q,k-1},$$

and the notation is such that the terms L_s represent quantities which are known or have already been computed, while the terms $u_{i,j,k}$, $v_{p,j,r}$, $w_{i,j,k}$, shown explicitly, are unknowns in the new time step.

After substituting (3.8) into (3.1)–(3.3) and combining these equations with (3.6) and (3.7), we shall have $3J$ equations, which are denoted by $\mathbf{E}_{3J}$, in $3J$ unknowns $\{(u,v,w)_j, j \in [1,J]\}$. These equations are nonlinear and their solution is obtained by Newton's method.

3.4. *Solution of the equations*

Newton's method, used in solving $\mathbf{E}_{3J}$, was found to be more accurate and at least as fast as the predictor–corrector fixed-point method which was tried initially. The rate of convergence of the Newton technique is of $O(\epsilon^{2^k})$, where ϵ is the initial difference between the true solution and the assumed solution, and k the number of iterations, while for the predictor–corrector fixed-point method, it is of $O(\epsilon)$. Thus, a solution of the nonlinear algebraic equations could be obtained with relatively few (usually 3 or 4) iterations. Some numerical experiments were performed using both methods and it was found that after 20 iterations only 6 or 7 digits were accurate using the predictor–corrector method, while the Newton technique gave 10 digits after 3 or 4 iterations, provided that a good initial guess was used. It should be noted that the amount of computation required for one iteration of each method is the same, the main difference being the amount of preliminary algebra required for the Newton technique, which is more than that for the predictor–corrector method.

Introduce the following notation, which suppresses indices which are not essential during the iterations:

$$U_j = u_{i,j,k}, \quad V_j = v_{p,j,r}, \quad W_j = w_{i,j,k}.$$

Let s denote the iterate and define the following iteration procedure:

$$(U, V, W)_j^s = (U_j^{s-1} + \delta U_j, V_j^{s-1} + \delta V_j, W_j^{s-1} + \delta W_j). \tag{3.9}$$

The $(U, V, W)_j$ are expressed in terms of the iterates as

$$(U, V, W)_j = \lim_{\{\delta U, \delta V, \delta W\}_j \to 0} (U, V, W)_j^s.$$

Substitute (3.9) into $\mathbf{E}_{3J}$ and retain first-order terms to $O(\delta U, \delta V, \delta W)_j$ to obtain the following equations:

$$P_j(\delta U_j + \delta U_{j-1}) + Q_j(\delta V_j - \delta V_{j-1}) + R_j(\delta W_j + \delta W_{j-1}) = T_j, \tag{3.10a}$$

$$A_j(\delta U_j + \delta U_{j-1}) + B_j(\delta V_j + \delta V_{j-1}) + C_j \delta W_j + D_j \delta W_{j-1} = E_j, \tag{3.10b}$$

$$F_j(\delta U_j - \delta U_{j-1}) + G(\delta W_j + \delta W_{j-1}) = H_j, \tag{3.10c}$$

where $2 \leqslant j \leqslant J$; the coefficients of $(\delta U, \delta V, \delta W)_j$, which depend on known quantities are given in Phillips (1972).

As a result of (3.6) and (3.7), we require

$$\delta U_1 = \delta V_1 = \delta U_J = 0. \tag{3.11}$$

Equations (3.10) and (3.11) represent $3J$ equations in the $3J$ unknowns $(\delta U, \delta V, \delta W)_j$, $1 \leqslant j \leqslant J$, and may be written in block matrix form (see Isaacson & Keller 1966, p. 58), but are more easily solved if we retain the algebraic notation. The system of equations is similar to the one studied by Ackerberg & Phillips (1972) and may be inverted by an efficient algorithm to be described below. First, we eliminate δW_j from (3.10) by the following steps.

(i) Rewrite (3.10a, b, c) with j replaced by $j+1$. Denote the result by (3.10a, b, c)′. (ii) Solve (3.10c) to obtain an equation for δW_j, denoted by (A). (iii) Solve (3.10c)′ to obtain an equation for δW_{j+1}, denoted by (B). (iv) Combining

(A) with (3.10b) to eliminate δW_j yields an equation for δW_{j-1}, denoted by (C). (v) Combine (A), (B), (C), (3.10a)′ and (3.10b)′ to eliminate δW_{j-1}, δW_j, δW_{j+1} and δV_{j+1} and we obtain the equation

$$A'_j\,\delta U_{j-1}+B'_j\,\delta U_j+C'_j\,\delta U_{j+1}+D'_j\,\delta V_j+E'_j\,\delta V_{j-1}=F'_j \quad \text{for} \quad 2\leqslant j\leqslant J-1. \tag{3.12}$$

(vi) Combine (C) with (A) to eliminate δW_j and δW_{j-1} from (3.10a) and we obtain the equation

$$P'_j\,\delta U_j+Q'_j\,\delta U_{j-1}+R'_j(\delta V_j-\delta V_{j-1})=S'_j \quad \text{for} \quad 2\leqslant j\leqslant J. \tag{3.13}$$

The coefficients in (3.12) and (3.13) are given in Phillips (1972).

Considering (3.11), (3.12) and (3.13), we have $2J$ equations in $2J$ unknowns which may be solved using the algorithm

$$\delta U_j=\alpha_j\,\delta U_{j-1}+\beta_j\,\delta V_{j-1}+\gamma_j \quad (2\leqslant j\leqslant J), \tag{3.14}$$

and (3.13) rewritten in the form

$$\delta V_j=\delta V_{j-1}+(R'_j)^{-1}(T'_j-Q'_j\,\delta U_{j-1}-P'_j\,\delta U_j) \quad (2\leqslant j\leqslant J). \tag{3.15}$$

Here

$$\alpha_j=[-A'_j+(R'_j)^{-1}Q'_j(C'_j\gamma_{j+1}+D'_j)]\,\mathscr{D}^{-1}, \tag{3.16a}$$

$$\beta_j=[F'_j-C'_j\beta_{j+1}-(R'_j)^{-1}S'_j(D'_j+C'_j\gamma_{j+1})]\,\mathscr{D}^{-1}, \tag{3.16b}$$

$$\gamma_j=-[C'_j\gamma_{j+1}+D'_j+E'_j]\,\mathscr{D}^{-1}, \tag{3.16c}$$

$$\mathscr{D}=B'_j+C'_j\alpha_{j+1}-(R'_j)^{-1}P'_j(C'_j\gamma_{j+1}+D'_j), \tag{3.16d}$$

for $2\leqslant j\leqslant J-1$.

The procedure may be started using (3.11) and choosing

$$\alpha_J=\beta_J=\gamma_J=0. \tag{3.17}$$

We then solve for the coefficients α_j, β_j and γ_j recursively, checking at each step that $\mathscr{D}\neq 0$. If $\mathscr{D}=0$, then the set of equations might be singular, but it is more likely that they can be rearranged to eliminate such a zero in the denominator. With the coefficients known, δU_j and δV_j may be found using (3.14) and (3.15) recursively, starting with values given by (3.11). δW_1 is next determined by writing (3.10b) and (3.10c) for $j=2$ and eliminating δW_2. Finally, δW_j, $2\leqslant j\leqslant J$, is determined using (3.10c).

The complete solution procedure is carried out in the plane $t=$ constant with the $(U, V, W)_j$ computed in succession along the lines $i=$ constant starting at $i=2$ and proceeding to $i=I$ (note that the initial condition in x is prescribed along $i=1$). Once an entire t plane is known, the next t plane can be computed, and the computation continued *ad infinitum* unless some difficulty develops, e.g. backflow.

As initial estimates for $(U, V, W)_j$ we used

$$U_j^0=u_{i,\,j,\,k-1} \quad (1\leqslant j\leqslant J), \tag{3.18a}$$

$$V_j^0=\begin{cases}0, & k=2\\ v_{i-\frac{1}{2},\,j,\,k-\frac{3}{2}}, & k\geqslant 3\end{cases} \quad (1\leqslant j\leqslant J) \tag{3.18b}$$

and

$$W_j^0=w_{i,\,j,\,k-1} \quad (1\leqslant j\leqslant J). \tag{3.18c}$$

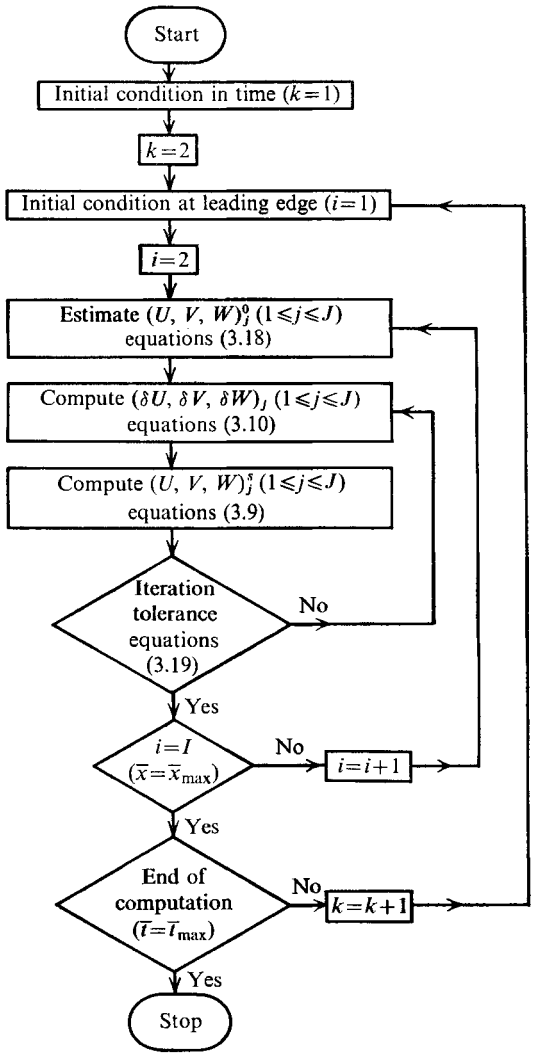

FIGURE 3. Computational flow chart.

The Newton iteration was stopped when

$$|\delta U_j/U_j^s|,\ |\delta V_j/V_j^s|,\ |\delta W_j/W_j^s| \leqslant \delta \quad (1 \leqslant j \leqslant J), \tag{3.19}$$

where δ is a small number (here $\delta = 0{\cdot}1 \times 10^{-10}$). The solution procedure is outlined in figure 3.

Since a set of quadratic equations must be solved to determine the $(U, V, W)_j$, a real unique solution is not guaranteed. When backflow is possible, it has been shown by Ackerberg (1965, p. 70) that, for the steady viscous flow inside a cone, two solutions of the boundary-layer equations are possible, one of which is rejected on physical grounds. The basis for assuming that the correct solution is obtained by the method proposed here is that flow quantities vary continuously from one station to the next. Moreover, when the initial values for $(U, V, W)_j^0$ were varied considerably, the same final results were obtained.

In an effort to reduce the number of iterations needed to solve the nonlinear equations, several initial guesses, other than (3.18), were used (Phillips 1972). However, these methods failed to reduce the number of iterations for the desired accuracy and were discarded since they involved more computation.

The numerical technique and computer programs were checked for their accuracy by solving the impulsively started flat-plate problem previously considered by Hall (1969*a*) and Dennis (1972), who used methods differing from that presented here. Our results were found to be in excellent agreement with theirs (Phillips 1972).

3.5. *The terms* L_s ($s = 1$–5)

No backflow. During part of the computation the boundary-layer flow is directed entirely downstream, with no backflow, and the finite-difference procedure is straightforward. In these cases we introduce the following second-order-accurate difference approximations in the known time plane $(t-\delta t)$:

$$u_{p,q,k-1} = \tfrac{1}{4}(u_{i,j,k-1} + u_{i,j-1,k-1} + u_{i-1,j,k-1} + u_{i-1,j-1,k-1}), \tag{3.20a}$$

with a similar expression for $w_{p,q,k-1}$,

$$(u_x)_{p,q,k-1} = (2\delta x_i)^{-1}(u_{i,j,k-1} + u_{i,j-1,k-1} - u_{i-1,j,k-1} - u_{i-1,j-1,k-1}) \tag{3.20b}$$

and

$$(w_\eta)_{p,q,k-1} = (2\delta\eta_j)^{-1}(w_{i,j,k-1} - w_{i,j-1,k-1} + w_{i-1,j,k-1} - w_{i-1,j-1,k-1}). \tag{3.20c}$$

Using (3.20), L_s ($s = 1$–5) can be evaluated in (3.8), thus determining each term in the finite-difference equations (3.10). Note that data from the i and $i-1$ grid lines in the $t-\delta t$ plane are required.

Backflow. With particles moving upstream, a finite-difference procedure should be used which allows particles flowing backwards to influence the flow upstream. To accomplish this the following difference approximation is used in the known time plane $(t-\delta t)$ which involves the $i-1$, i and $i+1$ grid lines when the i grid line is computed in the new time plane:

$$S_{p,q,k-1} = \frac{[(\delta x_i + \delta x_{i-1})\,S_{p+1,q,k-1} + (\delta x_i + \delta x_{i+1})\,S_{p-1,q,k-1}]}{\delta x_{i-1} + 2\delta x_i + \delta x_{i+1}}, \dagger \tag{3.21}$$

where

$$S_{p,q,k-1} \equiv (u, u_x, w, w_\eta)_{p,q,k-1}.$$

The values $S_{p,q,k-1}$ appearing on the right-hand side of (3.21) are evaluated using (3.20). This technique permits particles along x_{i+1} at $t-\delta t$ to influence the flow at x_i at t. Care must be taken that δt is sufficiently small so that particles along x_{i+1} at $t-\delta t$ do not influence the flow along x_{i-1} at t. This requires

$$|x_{i+1} - x_{i-1}| > |\min_j (u_{i+1,j,k-1}) \times \delta t_k|. \tag{3.22}$$

If (3.22) is violated, δt_k must be reduced sufficiently so that it holds. However, even if (3.22) holds, there is no guarantee that difficulty with the solution will be avoided. It would not be possible to compute flow quantities along the line

† This is not a simple average of $S_{p+1,q,k-1}$ and $S_{p-1,q,k-1}$ since we must account for the uneven mesh spacing in the x grid.

$i = I$ by this method without knowledge of the flow for $x > x_I$. It is fortunate, therefore, that the physics of the problem (see § 2.3) allows us to know the solution for $x \geqslant tU_{eM}$. Thus, the integration mesh is constantly expanded in the x direction so as to maintain $x_I > t_k U_{eM}$. It should be mentioned that, although the accuracy of the computation during the transient state could not be verified when there was backflow, the knowledge of the flow for $x > tU_{eM}$ allowed the computation to achieve the final periodic flow. Without a downstream condition, it was impossible to continue the numerical integration into a region of backflow owing to large oscillations.

Near the leading edge where backflow did not occur, this special method is not necessary and the finite-difference equations (3.20) may be used. Thus, depending on whether or not there is backflow, we use (3.21) or (3.20) to determine the quantities L_s, $s = 1$–5, in (3.8). This fully specifies the finite-difference method.

4. Periodic flow over a flat plate

4.1. *Formulation of the problem*

The governing equations are (2.3) and (2.4) with

$$U_e(t) = 1 + A \sin t \quad \text{and} \quad U_{eM} = 1 + A.$$

The boundary conditions in η and initial conditions in x are given by (2.5)–(2.7). We are interested in the periodic flow which evolves for $t \to \infty$. The problem was solved using two sets of initial conditions at $t = 0$, to illustrate that the final periodic flow is unique and does not depend on initial conditions. Here we give the initial condition used most often in our computations.

For $t = 0-$, we assume the flow is strictly periodic and corresponds to that over an infinite flat plate with $U_e = A \sin t$.† The problem is started by assuming that, in going from $t = 0-$ to $t = 0+$, we impulsively change from $U_e = A \sin t$ to $U_e = 1 + A \sin t$ and introduce the leading-edge condition (2.7); the velocity at all points $\bar{y} > 0$ will increase by unity and the initial condition (2.9) will be

$$u_0(x, \eta) = u_0(\xi) = 1 + A\, e^{-\xi} \sin \xi \quad \text{for} \quad \eta > 0, \tag{4.1}$$

where $\xi = \bar{y}[\bar{\omega}/2\bar{\nu}]^{\frac{1}{2}}$. From § 2.3 we have that, for $x \geqslant tU_{eM}$, the solution is independent of initial conditions at $x = 0$, and the problem represents the transient flow over an infinite flat plate with $U_e(t) = 1 + A \sin t$, subject to (2.5), (2.6) and (2.9) with u_0 given by (4.1). This solution, which is a function of $\bar{y}$ and $\bar{t}$, is expressed in terms of (x, η, t) as

$$\begin{aligned} \bar{u}(\bar{y}, \bar{t})/\bar{U}_e(\bar{t}) &= u(x, \eta, t) \\ &= U_e^{-1}\{\operatorname{erf}[\tfrac{1}{2}\eta(x/U_e t)^{\frac{1}{2}}] + A[\sin t - e^{-\xi} \sin(t - \xi)]\}, \end{aligned} \tag{4.2}$$

where $\xi = \eta(x/2U_e)^{\frac{1}{2}}$.

† Other flows may be assumed for $t = 0-$ (see Phillips 1972).

4.2. *Asymptotic solution for small x*

We seek a power-series expansion for small x. Our development follows the work of Moore (1951) except that here A is not assumed small. Introduce a stream function $F(x, \eta, t)$ such that

$$u = F_\eta, \quad v = \tfrac{1}{2}(\eta F_\eta - F) - xF_x. \tag{4.3}$$

We assume an expansion of the form

$$F = \sum_{n=0}^{\infty} x^n f_n(\eta, t). \tag{4.4}$$

After substituting (4.4) in (2.4), we find that the first few f_n may be written as

$$f_0 = R(\eta), \tag{4.5}$$

$$f_1(\eta, t) = U_e^{-2}\dot{U}_e g_1(\eta) \tag{4.6}$$

and

$$f_2(\eta, t) = U_e^{-3}\ddot{U}_e g_{2,1}(\eta) + (U_e^{-2}\dot{U}_e)^2 g_{2,2}(\eta). \tag{4.7}$$

Here $R(\eta)$ is the Blasius solution and the g's are solutions of the boundary-value problems

$$g_1''' + \tfrac{1}{2}Rg_1'' - R'g_1' + \tfrac{3}{2}R''g_1 = R' + \tfrac{1}{2}\eta R'' - 1, \tag{4.8}$$

$$g_{2,1}''' + \tfrac{1}{2}Rg_{2,1}'' - 2R'g_{2,1}' + \tfrac{5}{2}R''g_{2,1} = g_1' \tag{4.9}$$

and

$$g_{2,2}''' + \tfrac{1}{2}Rg_{2,2}'' - 2R'g_{2,2}' + \tfrac{5}{2}R''g_{2,2} = [g_1' - \tfrac{3}{2}g_1'' - 1]g_1' + \tfrac{1}{2}\eta g_1'' \tag{4.10}$$

subject to the boundary conditions

$$g(0) = g'(0) = 0 \tag{4.11}$$

and

$$g'(\eta) \to 0 \quad \text{for} \quad \eta \to \infty. \tag{4.12}$$

The method of finding numerical solutions is that used by Moore (1951) to solve similar equations. The numerical values for the second derivatives at the wall are

$$g_1''(0) = 0{\cdot}332057, \quad g_{2,1}''(0) = 0{\cdot}848522, \quad g_{2,2}''(0) = -0{\cdot}469687.$$

The expansion for small x may finally be written as

$$F(x, \eta, t) = R(\eta) + xU_e^{-2}\dot{U}_e g_1(\eta) + x^2[U_e^{-3}\ddot{U}_e g_{2,1}(\eta) + (U_e^{-2}\dot{U}_e)^2 g_{2,2}(\eta)] + O(x^3). \tag{4.13}$$

To obtain accurate results, the range over which x is allowed to vary in (4.13) should be restricted owing to the appearance of inverse powers of U_e. The largest coefficient of the x^n term is U_e^{-2n}, and to be certain that successive terms form a decreasing sequence, we require

$$x < \min(U_e^2).$$

4.3. *Results*

As an additional check on our numerical method and computer routines, a comparison was made with the 'small parameter' solution, which also required a numerical integration (see Ackerberg & Phillips 1972). Our computations were

x	δx	η	$\delta\eta$	t	$n\ (\delta t = 2\pi/n)$
$0{\cdot}0 \leqslant x < 0{\cdot}2$	0·1	$0{\cdot}0 \leqslant \eta < 0{\cdot}2$	0·05	$0 \leqslant t < \frac{1}{6}\pi$	96
$0{\cdot}2 \leqslant x < 0{\cdot}5$	0·15	$0{\cdot}2 \leqslant \eta < 1{\cdot}0$	0·1	$\frac{1}{6}\pi \leqslant t$	12
$0{\cdot}5 \leqslant x < 1{\cdot}0$	0·25	$1{\cdot}0 \leqslant \eta$	0·5	—	—
$1{\cdot}0 \leqslant x$	0·75	—	—	—	—

TABLE 1. Integration meshes used in computations for $A = 0{\cdot}1$.

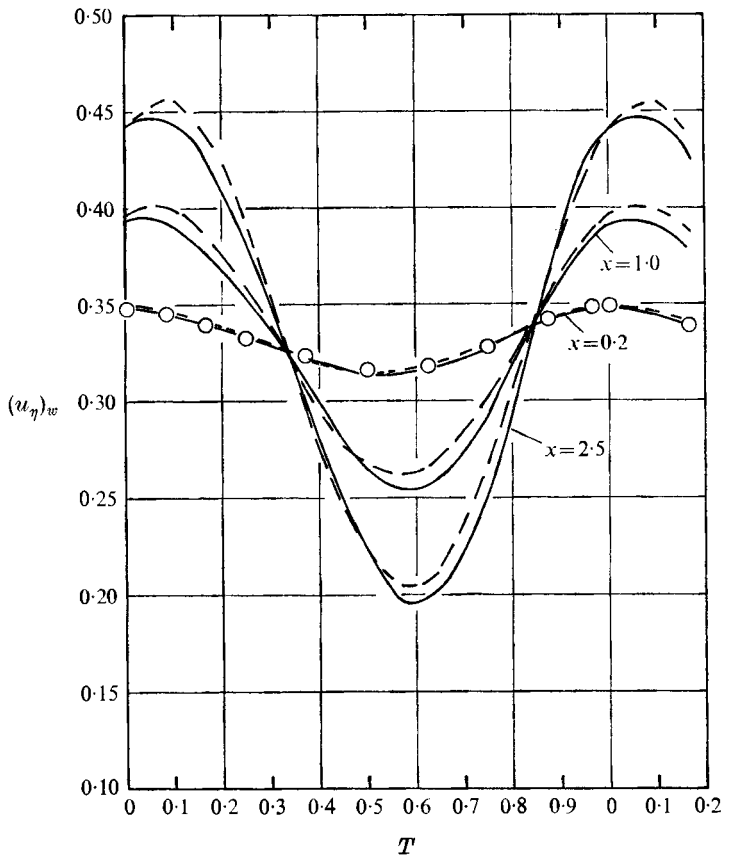

FIGURE 4. $(u_\eta)_w$ *vs.* T during third period, for $A = 0{\cdot}1$. —, numerical results; – – –, small parameter solution; ○, co-ordinate expansion for small x.

performed for $A = 0{\cdot}1$ with an integration mesh that is described in table 1. A plot of $u_\eta|_{\eta=0} = (u_\eta)_w$ *vs.* T, the fraction of a period, is presented in figure 4 for the third period of computation. The results of the co-ordinate expansion, valid for small x, are also shown for $x = 0{\cdot}2$. All results are in close agreement, and the maximum pointwise difference in $(u_\eta)_w$ between the numerical solution and the 'small parameter' solution is 3%, which is smaller than the nominal accuracy of the numerical technique.

For runs at larger values of A, for which backflow occurs within the computation grid, it was necessary to vary δt during the computation. If δt was chosen to

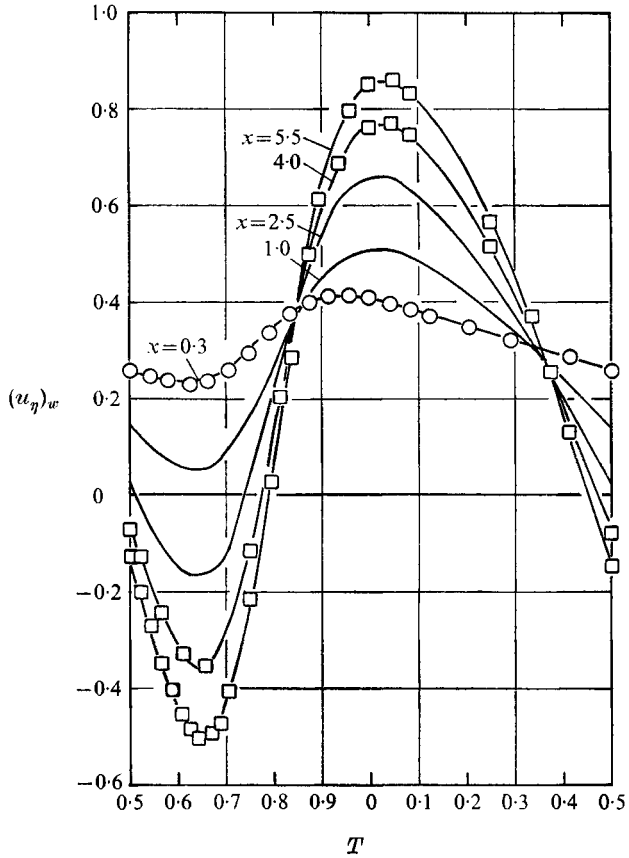

FIGURE 5. $(u_\eta)_w$ *vs.* T during fourth period, for $A = 0·3$. —, numerical results; O, co-ordinate expansion for small x; □, numerical results for previous period.

just satisfy (3.22), it did not seem possible to obtain accurate results. It was necessary to reduce δt considerably at the onset of backflow to prevent numerical oscillations which would otherwise appear in the solution and persist during the remainder of the computation. The amplitude of these oscillations increased with time until they were so large that Newton's iteration procedure would not converge after twenty iterations. If, however, δt was reduced, the oscillations disappeared in nearly all cases.

In figures 5–7, we show the results for a computation with $A = 0·3$. The integration mesh is described in table 2. A variable η mesh size was used to achieve better resolution in the region of backflow, which was close to the wall. The integrations were carried to $4\frac{1}{2}$ periods with a total running time of 352 s on the CDC 6600.

A plot of $(u_\eta)_w$ *vs.* T is shown in figure 5, with x represented parametrically. The results are for the fourth period of computation, with the third-period results indicated by squares to display the degree to which periodicity had been established. The difference in the values of $(u_\eta)_w$, for the two periods, is well below the nominal accuracy of the numerical method. The results from the co-ordinate

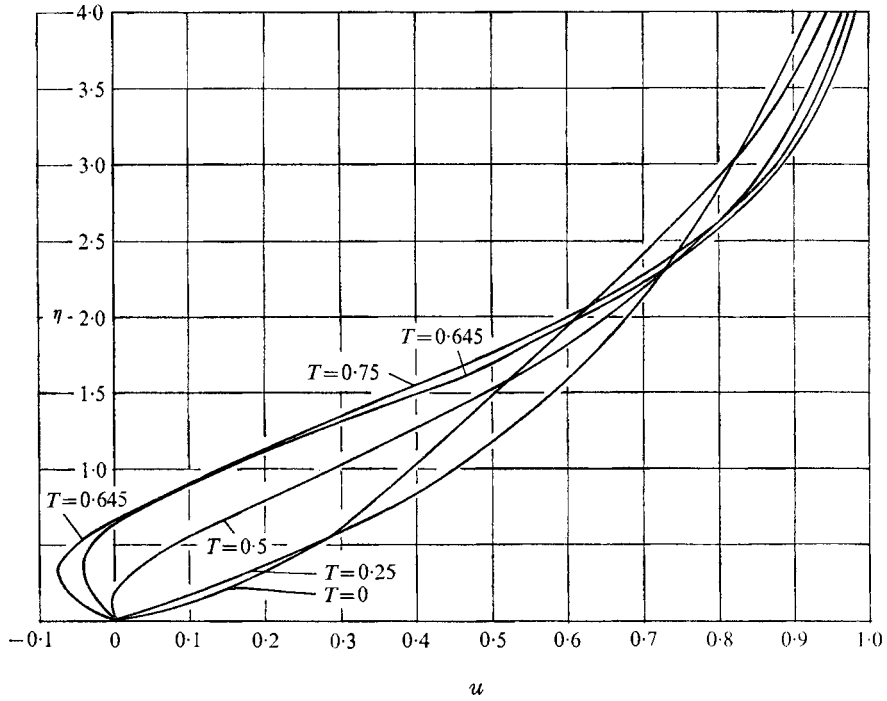

FIGURE 6. u *vs.* η; $x = 5{\cdot}5$, $A = 0{\cdot}3$. T is a parameter and the results are for the fourth period.

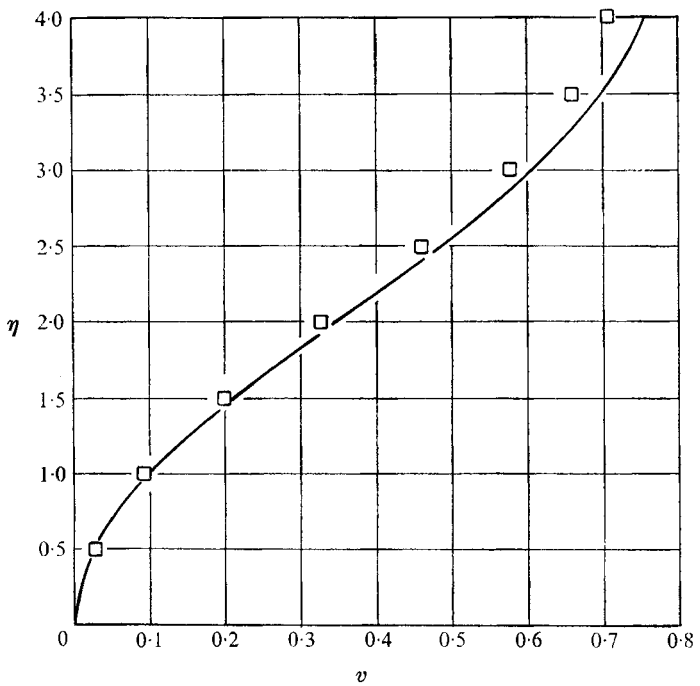

FIGURE 7. v *vs.* η; $x = 5{\cdot}125$, $T = 0{\cdot}6345$, during fourth period, for $A = 0{\cdot}3$. □, results for previous period.

x	δx	η	$\delta\eta$	t	n
$0{\cdot}0 \leqslant x < 0{\cdot}1$	0·1	$0{\cdot}0 \leqslant \eta < 0{\cdot}1$	0·025	$0 \leqslant t < \frac{1}{8}\pi$	96
$0{\cdot}1 \leqslant x < 0{\cdot}3$	0·2	$0{\cdot}1 \leqslant \eta < 0{\cdot}3$	0·05	$\frac{1}{8}\pi \leqslant t < \pi$	12
$0{\cdot}3 \leqslant x < 0{\cdot}4$	0·1	$0{\cdot}3 \leqslant \eta < 1{\cdot}0$	0·1	$\pi \leqslant t < 2\pi$	48
$0{\cdot}4 \leqslant x < 0{\cdot}5$	0·05	$1{\cdot}0 \leqslant \eta$	0·5	$2\pi \leqslant t < 3\pi$	12
$0{\cdot}5 \leqslant x < 1{\cdot}0$	0·25	—	—	$3\pi \leqslant t < 4\pi$	48
$1{\cdot}0 \leqslant x$	0·75	—	—	$4\pi \leqslant t < 5\pi$	12
				$5\pi \leqslant t < 6\pi$	48
				$6\pi \leqslant t < 7\pi$	24
				$7\pi \leqslant t < 8\pi$	96
				$8\pi \leqslant t < 9\pi$	24
				$9\pi \leqslant t$	96

TABLE 2. Integration meshes used in computations for $A = 0{\cdot}3$.

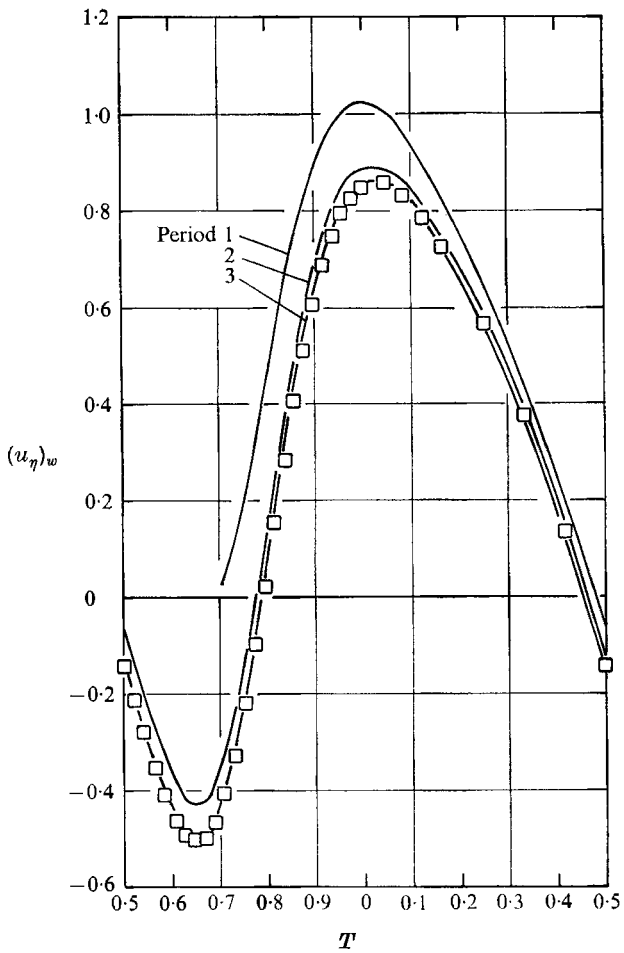

FIGURE 8. $(u_\eta)_w$ *vs.* T; $x = 5{\cdot}5$, $A = 0{\cdot}3$: the approach of the solution to its final periodic state. □, results for period 4.

expansion are indicated by circles for $x = 0{\cdot}3$, and the agreement is again close. The largest difference occurred near $T = 0{\cdot}75$, which corresponds to the minimum value of U_e and for which the neglected terms in (4.24) will be largest. Velocity profiles at $x = 5{\cdot}5$ are displayed in figure 6 for quarter periods and for $T = 0{\cdot}645$, which is the fraction of a period when maximum backflow is observed. A plot of v *vs.* η is presented in figure 7, for $T = 0{\cdot}6354$ and $x = 5{\cdot}125$. The v velocities are small in the region of backflow with the maximum value of about 0·8 occurring at the edge of the boundary layer. This seems to indicate that points of zero skin friction and regions of backflow for unsteady flow do not necessarily lead to any singular behaviour.

Figure 8, a plot of $(u_\eta)_w$ *vs.* T for the first four periods for $A = 0{\cdot}3$ and $x = 5{\cdot}5$, shows the transient approach of the solution to the final periodic state. It was found that the important criteria for the attainment of a periodic solution at a specific station, say x_0, is that $(tU_0/x_0) \sim 5$. For $x = 5{\cdot}5$ this is satisfied during the fifth period of computation. It is uncertain whether the transient solution displayed is accurate because we were unable to duplicate the transient results with any degree of satisfaction.

For these computations Richardson's extrapolation was not useful because, owing to the large computation times that would be involved, two runs could not be performed so that the extrapolated solution would be more accurate than the single most accurate run.

This paper was taken from a dissertation submitted to the Faculty of the Polytechnic Institute of Brooklyn in partial fulfilment of the requirements for the Ph.D. degree in Aeronautics and Astronautics (1972). Special thanks are due to the National Aeronautics and Space Administration for support given under the NASA Predoctoral Traineeship Program, and to the U.S. Army Research Office, Durham, under Grant no. DA-ARO-D-31-124-71-G68.

REFERENCES

Ackerberg, R. C. 1965 The viscous incompressible flow inside a cone. *J. Fluid Mech.* **21**, 47–81.

Ackerberg, R. C. & Phillips, J. H. 1972 The unsteady laminar boundary layer on a semi-infinite flat plate due to small fluctuations in the magnitude of the free-stream velocity. *J. Fluid Mech.* **51**, 137–157.

Ackerberg, R. C. & Phillips, J. H. 1973 A numerical method for highly accelerated laminar boundary-layer flows. *SIAM J. on Numerical Anal.* **10**, 147–160.

Dennis, S. C. R. 1972 The motion of a viscous fluid past an impulsively started semi-infinite flat plate. *J. Inst. Math. Applics.* **10**, 105–117.

Gibson, W. E. 1957 Ph.D. thesis, Massachusetts Institute of Technology.

Hall, M. G. 1969*a* The boundary layer over an impulsively started flat plate. *Proc. Roy. Soc.* A **310**, 401–414.

Hall, M. G. 1969*b* A numerical method for calculating unsteady two-dimensional laminar boundary layers. *Ing. Arch.* **38**, 97–106.

Isaacson, E. & Keller, H. B. 1966 *Analysis of Numerical Methods.* Wiley.

Keller, H. B. & Cebeci, T. 1971 Accurate numerical methods for boundary layer flows. Part 1. Two-dimensional laminar flows. *Proc. 2nd Int. Conf. on Numerical Methods in Fluid Dyn.* pp. 92–100. *Lecture Notes in Physics no.* 8. Springer.

LIGHTHILL, M. J. 1954 The response of laminar skin friction and heat transfer to fluctuations in the stream velocity. *Proc. Roy. Soc.* A **224**, 1–23.

LIN, C. C. 1957 Motion in the boundary layer with a rapidly oscillating external flow. *Proc. 9th Int. Cong. on Appl. Mech., Brussels*, **4**, 155–167.

MOORE, F. K. 1951 Unsteady laminar boundary-layer flow. *N.A.C.A. Tech. Note*, no. 2471.

PEDLEY, T. J. 1972 Two-dimensional boundary layers in a free stream which oscillates without reversing. *J. Fluid Mech.* **55**, 359–383.

PHILLIPS, J. H. 1972 Ph.D. thesis, Polytechnic Institute of Brooklyn.

SEARS, W. R. & TELIONIS, D. P. 1971 Unsteady boundary-layer separation. *Proc. IUTAM Symp. on Unsteady Boundary Layers*, pp. 404–447. Laval University, Quebec, Canada.

STEWARTSON, K. 1951 On the impulsive motion of a flat plate in a viscous fluid. *Quart. J. Mech. Appl. Math.* **4**, 182–198.

STEWARTSON, K. 1960 The theory of unsteady laminar boundary layers. In *Advances in Applied Mechanics*, Vol. 4, pp. 1–37. Academic.

TIKHONOV, A. N. & SAMARSKII, A. A. 1963 *Equations of Mathematical Physics*. Pergamon.